Supreet S. Bahga
Juan G. Santiago

Department of Mechanical Engineering, Stanford University, CA, USA

Received September 27, 2011
Revised November 14, 2011
Accepted November 24, 2011

Research Article

Concentration cascade of leading electrolyte using bidirectional isotachophoresis

We present a novel method of creating concentration cascade of leading electrolyte (LE) in isotachophoresis (ITP) by using bidirectional ITP. ITP establishes ion-concentration shock waves between high-mobility LE and low-mobility trailing electrolyte (TE) ions. In bidirectional ITP, we set up simultaneous shock waves between anions and cations such that these waves approach each other and interact. The shock interaction causes a sudden decrease in LE concentration ahead of the focused anions and a corresponding decrease in analyte zone concentrations. This readjustment of analyte zone concentrations is accompanied by a corresponding increase in their zone lengths, in accordance to conservation laws. The method generates in situ gradient in the LE concentration, and therefore can be achieved in a single, straight channel simply by establishing the initial electrolyte chemistry. We have developed an analytical model useful in designing the process for maximum sensitivity and estimating increase in sample zone length due to shock interaction. We also illustrate the technique and evaluate its effectiveness in increasing detection sensitivity using transient simulations of species transport equations. We validated the theoretical predictions using experimental visualizations of bidirectional ITP zones for various electrolyte chemistries. Lastly, we use our technique to demonstrate a factor of 20 increase in the sensitivity of ITP-based detection of 2,4,6-trichlorophenol.

Keywords:
Bidirectional isotachophoresis / Cascade isotachophoresis / Concentration shock waves / Detection sensitivity / Shock interaction DOI 10.1002/elps.201100510

1 Introduction

Isotachophoresis (ITP) is an electrophoresis-based technique that preconcentrates and separates ionic species into distinct zones based on their electrophoretic mobilities. In ITP, analytes simultaneously focus and separate between zones of high effective mobility leading electrolyte (LE) ions and low effective mobility trailing electrolyte (TE) ions [1, 2]. Adjacent zones in ITP are separated by sharp zone boundaries, which result from a balance between electromigration and diffusive fluxes. These zone boundaries are self-sharpening in nature due to nonlinearity in the electromigration flux, and therefore can be described as ion-concentration shock waves [3, 4].

Correspondence: Professor Juan G. Santiago, Department of Mechanical Engineering Stanford University, 440 Escondido Mall, Bldg 530, room 225, Stanford, CA 94305, USA
E-mail: juan.santiago@stanford.edu
Fax: 650-723-7657

Abbreviations: LE, leading electrolyte; **NFT**, nonfocusing tracer; **PVP**, polyvinylpyrrolidone; **TE**, trailing electrolyte; **TCP**, 2,4,6-trichlorophenol

In ITP, analytes present in sufficient amounts will focus and segregate into distinct plateau-like zones with locally uniform concentrations. This ITP mode is called "plateau mode" ITP [5] as it is characterized by relatively long zones of locally uniform concentrations separated by thinner zone boundaries. For trace quantities, analyte species may not develop into such plateaus. Instead, multiple trace analyte species bounded by TE and LE focus into nearly completely overlapping peaks whose widths are governed by the diffuse TE-to-LE interface. This regime is termed "peak mode" ITP [5, 6]. Unlike plateau mode ITP, two adjacent zones in peak mode are practically indistinguishable from each other. Of course, a system with multiple analytes with a wide range of concentrations can form a "mixed mode" ITP condition. In mixed mode, depending upon their amounts, some analytes form peaks while others form plateaus (see, e.g., Fig. 1C in Ref. [7]).

Plateau mode ITP allows separation and detection of multiple analytes. Methods of analyte detection include a wide range of physicochemical properties, such as local conductivity [8], UV absorbance [9], and temperature [1]. Alternatively, the displacement physics of plateau mode ITP can be

Color Online: See the article online to view Figs. 1–3 in Color.

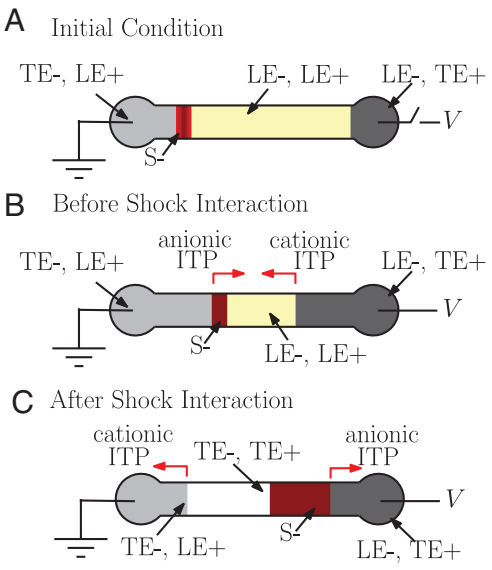

Figure 1. Schematic illustrating increase in analyte zone length upon shock interaction in bidirectional ITP. (A) The channel is initially filled with a mixture of LE+ and LE−. The reservoir on the left is filled with TE−/LE+ mixture, and the reservoir on the right is filled with LE−/TE+ mixture. Sample ions S− can be injected between the LE− and TE− zones. Buffers are chosen such that LE+ and TE+ are cations of weak bases and have, respectively, high and low absolute mobility. LE− and TE− are anions with effective mobility higher and lower than that of S−, respectively. (B) When voltage is applied, the anionic analyte (S−) focuses between LE− and TE− and the analyte zone propagates toward the right. Simultaneously, a leftward-propagating cationic ITP shock forms between LE+ and TE+. (C) When the cationic ITP shock interacts with the analyte zone, the LE zone transitions from LE−/LE+ to LE−/TE+. Electrolytes are chosen such that LE− concentration is significantly lower in LE−/TE+ zone than in LE−/LE+ zone. The ITP focusing physics therefore dictates that analyte concentration drops (to balance electromigration flux and maintain electroneutrality). This decrease in the S− concentration is accompanied by a strong increase in sample zone length, significantly increasing the detection sensitivity.

leveraged to detect analyte zones using indirect detection techniques, as in the fluorescent nonfocusing tracer (NFT) technique [10]. Typical isotachopherograms obtained from all of these measurement methods consist of steps in the measured quantity (e.g., conductivity or fluorescence) corresponding to different ITP zones. The width of these steps is proportional to the amount of focused analytes, and the ability to detect trace amount of analytes is limited by the step width relative to the thickness of diffused boundaries. Therefore, signal -to-noise ratio in plateau mode ITP can be defined as the length of analyte zone normalized by the characteristic length of diffusive zone boundaries [11, 12].

The sensitivity of plateau mode ITP detection is improved by increasing plateau zone width relative to the diffusive length of interfaces. As described by Garcia-Schwarz et al. [13], interface widths scale inversely with electric field and can be affected by advective dispersion and the mobility difference between co-ions in neighboring ITP zones. Several methods exist that can be used to increase the zone lengths in plateau mode ITP. These include (i) longer separation channels, (ii) the application of hydrodynamic counterflow [14], (iii) using channels with converging cross-sections [15–18], and (iv) using concentration cascade of the LE in the so-called "cascade ITP" technique [19]. All these techniques favor a longer sample accumulation time prior to the detection, and thereby increase plateau zone lengths. Longer analysis time also increases the separation capacity [20] of the system as analytes in the initial mixture have longer time to separate into purified zones [2, 19]. The basic principles of the aforementioned techniques and the necessary instrumentation have been reviewed elsewhere [2]. All or some of these techniques can be coupled to increase detection sensitivity, largely without affecting their individual performance. Therefore, these techniques can be studied and optimized independently before their integration.

In ITP, the concentrations of plateau zones scale proportionally to the concentration of the LE ions. Analytes can be said to "adjust" to a concentration established by that of the LE and an order unity (typically <1.0) multiplier associated with the system's ion mobilities [21, 22]. Cascade ITP [2] leverages this feature by focusing analytes sequentially using two LE zones. Analytes are first focused using a high concentration LE that increases sample loading and separation capacity; subsequently, analytes are detected using a low concentration LE. Analyte zones migrate from regions formerly occupied by the first LE into regions formerly occupied by the second LE and, as they do so, their concentration adjusts to a lower value set by the low concentration LE. This adjustment is accompanied by a corresponding increase in analyte zone lengths, in accordance to the mass conservation of species. Cascade ITP was first introduced by Bocek et al. [19], who used two LEs with a concentration ratio of 5:1 to enhance the separation of orthophosphate and pyrophosphate ions. Later, Kaniansky et al. [23] demonstrated on–chip integration of this technique and showed conductivity-based detection of several anions, including nitrate, chloride, and fluoride ions. To our knowledge, all previous work on cascade ITP required preset, physical separations between zones of high and low concentration LE. This separation has been accomplished using a column coupling arrangement (basically a T–junction) [23] and often controlled with valves [19]. These requirements complicate the application of cascade ITP and have excluded the integration of cascade ITP into a simple, single-channel architecture. These requirements also require an actuation step (of electrodes and/or valves) midway into the assay.

We here present a novel method of creating a concentration cascade of LE. Our method requires no actuation and can be achieved in a single, straight channel system. We effectively "chemically" transition from one LE to another by using bidirectional ITP. Bidirectional ITP involves simultaneous anionic and cationic ITP in a single channel and is characterized by anionic and cationic ITP shocks propagating either toward or away from each other [24, 25]. In the current work, we use a bidirectional ITP mode where the anionic and cationic shock waves approach each other and interact to modify the electrophoresis conditions [26]. Prior

to shock wave interaction, analytes are subjected to a relatively high concentration LE. Shock wave interaction then causes a sudden decrease of the LE ion concentration in the region ahead of the focused analytes. The technique can be used with either anionic or cationic ITP, removes the requirement of physical separation of LEs, and can be "programmed" into a cascade ITP process in a single, straight channel by setting the initial electrolyte chemistry.

We begin the paper by describing our method of creating a concentration cascade of LE using bidirectional ITP. We then present an analytical model to predict the increase in zone length due to shock interaction and to help in selection of electrolyte chemistry for maximum detection sensitivity. We also present detailed numerical simulations to illustrate our technique. We confirm these simulations using experimental visualization of cascade ITP process in bidirectional ITP. We then present a series of controlled bidirectional ITP experiments with various electrolytes that show maximized detection sensitivity. Lastly, we employ our technique for the high-sensitivity, indirect fluorescence based detection of 2,4,6-trichlorophenol (TCP) (a carcinogenic pollutant).

2 Materials and methods

2.1 Concept of creating concentration cascade of LE using bidirectional ITP

Bidirectional ITP involves simultaneous anionic and cationic ITP and is characterized by anionic and cationic ITP shock waves that propagate in opposite directions. Bidirectional ITP experiments require two oppositely charged pairs of LE and TE ions, which we here term as LE+, TE+, LE−, and TE−. LE and TE again denote the leading and TE ions, respectively, and + and − correspond to cations and anions, respectively. Depending on the initial conditions, shocks in bidirectional ITP can be made to propagate either toward or away from each other. In the former mode, anionic and cationic ITP shocks eventually interact and result in the formation of new ITP zones. Electrophoretic conditions in these newly created zones can differ markedly from those prior to the shock interaction. For example, shock interaction can change the identity of the counterion species, the concentration of co-ion species, local ionic strength, and pH, and this can quickly establish new focusing or separation conditions for analytes.

In the current work, we use shock interaction in bidirectional ITP to initiate a decrease in concentration of LE− ions and thereby elongate the zones of focused anionic analytes (consistent with cascade ITP). That is, prior to the shock interaction we focus anions with a high concentration LE− and then have shock interaction suddenly decrease the concentration of LE− ahead of the focused anions. Under these modified ITP conditions, the focused analyte zones are forced to readjust to lower concentrations. This decrease in the concentration of analyte zones is accompanied by a corresponding increase in the zone lengths. Although we here explore anionic ITP, in general our technique is equally applicable for increasing the sensitivity of cationic ITP by effecting a change in LE+ concentration.

Figure 1 shows a schematic of our technique. We first fill a straight channel with a mixture of LE+ and LE−, as shown in Fig. 1A. We empty and then fill the reservoir on the left with a mixture of TE− and LE+. Similarly, we empty and then fill the reservoir on the right with a mixture of TE+ and LE−. LE− and LE+ serve as the LE ions for anionic and cationic ITP, respectively, whereas, TE− and TE+ serve as TE ions for anionic and cationic ITP, respectively. We inject the analyte ions, S−, between the LE− and TE− zones. As shown in Fig. 1B, when voltage is applied along the channel, S− ions focus between the LE− and TE− ions and migrate rightwards. Simultaneously, a cationic ITP shock (LE+/TE+ interface) forms near the right reservoir and migrates leftwards. To create a concentration cascade in LE−, we choose our electrolytes such that the concentration of LE−, the counterion for cationic ITP, drops significantly behind the cationic ITP shock (in the LE−/TE+ zone). Subsequently, when the cationic ITP shock meets the focused anionic analyte zone, LE−/TE+ zone replaces the LE−/LE+ zone as the LE for anionic ITP. The low concentration of LE− in the LE−/TE+ zone compared to the LE−/LE+ zone causes the analyte zone to readjust to lower concentration. Consequently, the analyte zone length increases significantly (Fig. 1C). Later in Section 3.2, we discuss and quantify the choices of electrolyte chemistries that control and help maximize the zone length after the shock interaction.

In our technique, the cationic ITP does not affect the initial focusing of analyte ions in anionic ITP. The purpose of cationic ITP is to automatically trigger a change from high to low LE− concentration via shock interaction. In this way, our technique differs significantly from traditional cascade ITP wherein two unidirectional anionic ITP processes with different LE− concentration are coupled physically via valves [19] or a column coupling arrangement [23]. In other words, in traditional cascade ITP, the gradient in LE− concentration is realized by using bulk flow to establish two distinct regions in space that have different values of the regulating function (Kohlrausch [21] or Jovin-Alberty [22, 27]), as determined by two independent chemical mixtures. In contrast, our technique uses interaction with a cationic ITP interface to effect a temporal change of the LE− concentration, while keeping the regulating function constant (and equal to the value set initially by the LE−/LE+ mixture in the channel).

We note our technique also differs markedly from previous applications of bidirectional ITP with approaching shock waves. Bidirectional ITP with approaching shock waves was introduced by Oshurkova and Ivanaova [28], who used it to measure the conductivity of a binary electrolyte consisting of LE− and LE+ ions. However, their analysis was limited to states of the system prior to shock interaction (namely the analysis of rate at which the shock waves approach). We know of no study, other than that by Bahga et al. [26], where shock interaction in bidirectional ITP has been used to couple two electrophoretic processes. Bahga et al. used the changes in ITP focusing conditions associated with shock interaction to

couple ITP preconcentration with capillary electrophoresis (CE). Here, we present a new use of shock interaction in bidirectional ITP for effecting cascade ITP.

We also note our scheme is compatible with both "finite" and "semi-infinite" injection schemes [5, 11]. In Fig. 1, we show a finite sample injection scheme wherein sample ions are initially sandwiched between LE−/LE+ and TE−/LE+ zones. Alternatively, to increase sensitivity and minimize complexity, sample ions can be mixed with the TE−/LE+ mixture and allowed to focus continuously over time. In both cases, ITP focusing with high LE− concentration allows for greater sample loading prior to detection in the region formerly occupied by the low LE− concentration. We emphasize that an increase in lengths of anionic ITP zones occurs primarily due to the decrease in LE− concentration across the cationic ITP shock. Therefore, the injection method has no effect on the increase in zone length due to shock interaction. To illustrate these injection methods, we will here use both finite and semi–infinite injection schemes for our experiments (see Sections 3.4–3.6).

2.2 Materials and instrumentation

We performed experiments to visualize and quantify the increase in analyte zone lengths due to concentration cascade of LE in bidirectional ITP. We used the fluorescent NFT technique [10] for simultaneous visualization of all bidirectional ITP zones. For these visualization experiments, LE− was 100 mM Mops, TE− was 20 mM Taurine, LE+ was 280 mM Imidazole, and TE+ was 100 mM Bistris. We used Hepes and Tricine as model anionic analytes. We used a similar protocol as shown schematically in Fig. 1. To inject finite amounts of analytes, we first added Hepes and Tricine to the TE−/LE+ mixture at a concentration of 0.5 and 1 mM, respectively. We then allowed these analytes to focus until the analyte zones moved 5 mm from the TE− well. Subsequently, we replaced the mixture of analytes and TE−/LE+ with pure TE−/LE+, to effect a finite injection. We describe the injection protocol in more detail in the Supporting Information. We used a similar electrolyte chemistry and injection protocol for experiments demonstrating the effect of electrolyte composition on analyte zone length (Section 3.5). There, we adjusted the composition of LE−/LE+ mixture by fixing the concentration of LE− at 100 mM and changing LE+ concentration from 200 to 320 mM.

For the experiments demonstrating focusing and detection of TCP, we used 150 mM Mes as LE−, 20 mM Hepes as TE−, 470 mM imidazole as LE+, and 300 mM Bistris as TE+. To increase the sample loading by continuously focusing the sample, we mixed TCP with TE−/LE+ mixture (diluted from 1 mM stock).

To visualize zones in all experiments, we prepared 1 mM stock solution of the Alexa Fluor 488 dye (Invitrogen, Carlsbad, CA, USA) and used it as a fluorescent NFT by mixing at a concentration of 25 μM in the TE−/LE+ mixtures. We prepared 1 M stock solutions of Mops, Mes, Tricine, Hepes, Imidazole, Bistris, and 200 mM solution of Taurine before diluting them to the desired concentrations in different solutions. We added 1% w/w polyvinylpyrrolidone (PVP) to all solutions to suppress electroosmotic flow (EOF). All chemicals were obtained by Sigma-Aldrich (St. Louis, MO, USA) and were prepared in UltraPure DNase/RNase-free distilled water (GIBCO Invitrogen).

We captured images using an inverted epifluorescent microscope (IX70, Olympus, Hauppauge, NY, USA) equipped with a light-emitting diode lamp (LEDC1, Thor Labs, Newton, NJ, USA), U-MWIBA filter-cube from Olympus (460–490 nm excitation, 515 nm emission, and 505 nm cut off dichroic), and 2× (NA = 0.08) and 10× (NA = 0.3) objectives (Olympus). Images were captured using a 12 bit, 1300 × 1030 pixel array charge-coupled device (CCD) camera (Micromax1300, Princeton Instruments, Trenton, NJ, USA). We controlled the camera using Winview32 (Princeton Instruments) and processed the images with MATLAB (R2007b, Mathworks, Natick, MA, USA). We conducted the experiments by applying either constant voltage or current using a sourcemeter (model 2410, Keithley Instruments, Cleveland, OH, USA).

All experiments were performed on off-the-shelf Caliper NS 12A borosilicate glass microchips from Caliper Life Sciences (Mountain View, CA, USA). These microchips have channels wet etched to a depth of 20 μm with a mask width of 50 μm. In the Supporting Information, we show a schematic of the microchip and injection protocol. Although the chip consisted of four channels in a cross-geometry, we applied electric field only along one channel (53 mm long) for our experiments. We filled the North, South, and East reservoirs of the chip with LE−/LE+ mixture and applied vacuum to the West reservoirs until all channels were filled. We then rinsed the East and the West reservoirs with distilled water and filled them with cationic and anionic TE solutions, respectively.

3 Results and discussion

3.1 Theory of cascade ITP

In ITP, analytes focus between LE and TE zones under applied electric field only if their electrophoretic mobilities are less than that of LE ions in the LE zone and greater than TE ions in the TE zone. When present in large quantities, analytes in ITP focus and segregate into plateau-like zones, whose concentrations are directly proportional to the LE ion concentration [21, 22]. Thus, for a fixed amount of focused analyte, zone length (Δ) is inversely proportional to the LE ion concentration (c_L). Furthermore, irrespective of the injection scheme, the maximum amount of sample which can be focused (load capacity, N_a) is proportional to the LE ion concentration [5, 20]. For maximum attainable zone length in ITP, the effects of LE ion concentration on load capacity and the analyte zone concentration therefore cancel since

$$N_a \propto c_L, \quad \Delta \propto \frac{N_a}{c_L}. \tag{1}$$

Therefore, in ITP with uniform LE concentration, the maximum achievable zone length does not change with LE concentration. However, in cascade ITP, this limitation does not exist since load capacity is determined by the high concentration LE, while analyte zone concentration during detection is governed by the low concentration LE.

In cascade ITP, analytes first focus behind high concentration LE that allows for higher sample loading ($N_a \propto c_{L,high}$). The analyte zones are subsequently detected in a region following LE at low concentration, where the analyte zone concentrations are proportional to the lower LE concentration ($c_{L,low}$). The maximum zone length of focused analytes in cascade ITP, therefore, scales with the ratio of high to low LE concentrations,

$$N_a \propto c_{L,high}, \quad \Delta \propto \frac{N_a}{c_{L,low}}, \quad \Delta \propto \frac{c_{L,high}}{c_{L,low}}. \tag{2}$$

Further, in cascade ITP, for a fixed amount of analyte focused between the LE and TE zones, the ratio of analyte zone length in the high and low concentration LE is given by, $\Delta_{after}/\Delta_{before} = c_{L,high}/c_{L,low}$. Here, subscripts *before* and *after* denote the state of analyte zones in regions formerly occupied by high and low LE concentrations, respectively. Thus, the increase in zone length due to the transition of analyte zone is set simply by the concentrations of the two LEs.

3.2 Prediction of increase in zone length in bidirectional ITP

Unlike conventional cascade ITP, the gradient in LE concentration in our technique (shown in Fig. 1) is generated in situ. Therefore, the increase in zone length in our technique is not known directly from the initial conditions. To study the effect of shock interaction on analyte zone lengths, we here develop a simplified model for bidirectional ITP with interacting shocks. Knowing the composition of initial LE−/LE+ mixture and the species mobilities, our model predicts the concentrations of analyte zones before and after the shock interaction. The change in analyte zone concentration due to shock interaction can then be related to the change in the zone lengths.

We begin by considering an electrolyte system consisting of N chemical species. We assume safe pH conditions ($5 < \text{pH} < 9$, [4]) and that all species are univalent acids or bases. We note these conditions are satisfied by the experiments presented in Sections 3.4–3.6. For simplicity, we neglect the effect of ionic strength on electrophoretic mobilities of species (later in Section 3.3, we show detailed numerical simulations where we include the effects of ionic strength on species mobilities). Under these assumptions, we can use the conservation functions (also known as regulating functions) derived by Jovin [27] and Alberty [22] to relate species concentrations in different bidirectional ITP zones to the initial concentrations of LE− and LE+. For Nspecies, the Jovin function, $J(x,t)$, and the Alberty function, $A(x,t)$, can be written as,

$$J(x,t) = \sum_{i=1}^{N} z_i c_i(x,t) = J(x,0),$$

$$A(x,t) = \sum_{i=1}^{N} \frac{z_i c_i(x,t)}{\mu_i^0} = A(x,0). \tag{3}$$

Here, z_i, c_i, and μ_i^0, respectively, denote the valence, total (analytical) concentration, and absolute mobility of species i. Throughout, we use c_i to denote the total concentration (analytical concentration) of species i, defined as the sum total of concentrations of all ionization states belonging to species i [29]. Mobility is here defined the ratio of actual drift velocity to local electric field, a signed quantity. The superscript 0 in mobility refers to the absolute mobility, defined as the species mobility when fully ionized at zero ionic strength [30]. Eliminating the concentration of Nth species from the Jovin and Alberty functions defined in Eq. (3), we define a "combined Jovin-Alberty conservation function,"

$$F(x,t) = \sum_{i=1}^{N-1} \left(\frac{1}{\mu_i^0} - \frac{1}{\mu_N^0} \right) z_i c_i(x,t) = F(x,0). \tag{4}$$

We now use this conservation function, $F(x,t)$, to determine concentrations of analyte zones before and after the shock interaction.

As shown in Fig. 1A, initially, the channel is filled with the LE−/LE+ mixture, which alone sets the value of combined Jovin–Alberty function throughout the channel. When electric field is applied, S− ions displace LE− ions and their concentration adjusts to the value of $F(x,t)$ set by the LE−/LE+ mixture (Fig. 1B). Using LE+ as the Nth species in Eq. (4), we obtain the concentration of focused analyte before the shock interaction ($c_{S-,before}$)in terms of the initial LE− concentration ($c_{L-,init}$),

$$\left(\frac{1}{\mu_{S-}^0} - \frac{1}{\mu_{L+}^0} \right) c_{S-,before} = \left(\frac{1}{\mu_{L-}^0} - \frac{1}{\mu_{L+}^0} \right) c_{L-,init}. \tag{5}$$

Here, subscripts $S-$, $L-$,and $L+$ denote analyte, LE− and LE+ ions, respectively. The second subscript *init* denotes the value set by the initial conditions. When the anionic and cationic ITP shocks interact, TE+ replaces LE+ as the counter–ion for anionic ITP (see Fig. 1C). To obtain the concentration of analyte after the shock interaction, $c_{S-,after}$,we choose TE+ (denoted by $T+$) as the Nth species in Eq. (4),

$$\left(\frac{1}{\mu_{S-}^0} - \frac{1}{\mu_{T+}^0} \right) c_{S-,after} = \left(\frac{1}{\mu_{L-}^0} - \frac{1}{\mu_{T+}^0} \right) c_{L-,init} - \left(\frac{1}{\mu_{L+}^0} - \frac{1}{\mu_{T+}^0} \right) c_{L+,init}^0. \tag{6}$$

Equations (5) and (6) give the expressions for analyte zone concentrations before and after the shock interaction in terms of the species mobilities and the initial concentrations of LE+

($c_{L+,init}$), and LE− ($c_{L-,init}$). For a fixed amount of accumulated sample, the gain in zone length due to shock interaction is, therefore, given by,

$$\frac{\Delta_{after}}{\Delta_{before}} = \frac{c_{S-,before}}{c_{S-,after}} = \left(\frac{1-\mu^0_{L+}/\mu^0_{L-}}{1-\mu^0_{L+}/\mu^0_{S-}}\right)\left(\frac{1-\mu^0_{T+}/\mu^0_{S-}}{1-\mu^0_{T+}/\mu^0_{L-}}\right) \times \left[1-\frac{c_{L+,init}}{c_{L-,init}}\left(\frac{1-\mu^0_{T+}/\mu^0_{L+}}{1-\mu^0_{T+}/\mu^0_{L-}}\right)\right]^{-1}. \quad (7)$$

The three parenthetic expressions in this relation for $\Delta_{after}/\Delta_{before}$ are the ratios $c_{S-,before}/c_{L-,init}$, $c_{L-,after}/c_{S-,after}$, and $c_{L-,init}/c_{L-,after}$, respectively. In typical ITP experiments, the ratio of LE concentration to the corresponding analyte zone concentration is order unity. Therefore, the first two terms in Eq. (7) do not contribute, significantly, to the increase in zone length, and the expression for $\Delta_{after}/\Delta_{before}$ in Eq. (7) can be approximated as

$$\frac{\Delta_{after}}{\Delta_{before}} \approx \left[1-\frac{c_{L+,init}}{c_{L-,init}}\left(\frac{1-\mu^0_{T+}/\mu^0_{L+}}{1-\mu^0_{T+}/\mu^0_{L-}}\right)\right]^{-1}. \quad (8)$$

In other words, the change in zone length is primarily due to the ratio of LE− concentrations across the cationic ITP shock, and to a lesser extent due to the change in counter-ion from LE+ to TE+ upon shock interaction. Equation (8) is useful to quickly and approximately evaluate the effectiveness of electrolyte chemistry in increasing the detection sensitivity via shock interaction. For example, choosing $c_{L+,init}/c_{L-,init} = 3$, $\mu^0_{T+}/\mu^0_{L+} = 2/5$, and $\mu^0_{T+}/\mu^0_{L-} = -1$, by Eq. (8) yields up to 10-fold increase in the zone length due to shock interaction.

The analytical expression for increase in zone length given by Eq. (8) allows us to derive guidelines for choosing electrolyte chemistry to maximize the detection sensitivity. First, the gain in zone length increases by increasing the proportion of LE+ in the initial LE−/LE+ mixture, that is, higher $c_{L+,init}/c_{L-,init}$ ratio. Second, choosing TE+ as a weak base with a very low absolute mobility compared to that of LE+ (lower μ^0_{T+}/μ^0_{L+}ratio) favors longer analyte zones after the shock interaction. When these two conditions are satisfied, the higher value of the total LE+ concentration in the LE−/LE+ mixture causes TE+ to adjust to a high total concentration relative to the approximately fully ionized LE− concentration. That is, TE+ is then a weak base that is only partially ionized behind the LE+/TE+ interface at these conditions. As a result, the conductivity of TE+ zone drops significantly and the local electric field correspondingly jumps to a significantly higher value behind the LE+/TE+ interface. Choosing TE+ with very low absolute mobility also promotes this by further lowering local conductivity behind the cationic ITP shock. The high local electric field in the LE−/TE+ zone is consistent with a strong decrease of LE− concentration, in accordance with the continuity of electromigration flux across the cationic ITP shock. As the shocks interact, the LE−/TE+ mixture with low LE− concentration replaces the initial LE−/LE+ mixture as the LE for anionic ITP. This causes anionic ITP zones to readjust to lower LE− concentrations and longer lengths. This achieves cascade ITP automatically and robustly with absolutely no actuation (such as voltage changes, electric switches, or valves).

We here provide some examples of viable electrolyte chemistries for our technique. These can be used to increase the sensitivity of anionic ITP by just modifying the initial electrolyte chemistries. The key requirements are that LE+ concentration should be high compared to LE− concentration and TE+ ions should have very low absolute mobility compared to LE+ ions. Since the required concentrations of LE+ and TE+ in our method are higher than those of anionic species, we choose LE+ and TE+ as weak bases so as to keep the ITP zones well buffered. Several choices exist for high- and low-mobility weak bases applicable as LE+ and TE+, respectively. Table 1 shows three practical choices each for LE+ and TE+, combination of which yield nine unique cationic ITP chemistries. On the other hand, there are no specific constraints on LE− and TE− except the usual requirements on species mobilities for focusing anions in anionic ITP.

To obtain the analytical expression for increase in zone length (Eq. (7), we have neglected the effect of ionic strength on species mobilities. However, ITP experiments are generally performed at higher ionic strengths (10–100 mM range) to achieve significant buffering capacity. Therefore, the analytical model presented above is strictly valid only in the limit of zero ionic strength, and should be used only for qualitative electrolyte selections and rough predictions of the effect of electrolyte chemistry on the zone length. For more quantitative estimates of zone length, it is necessary to couple a model of ionic strength effects on species mobility with ITP dynamics.

In the current work, we use the SPRESSO simulation tool [31, 32] to solve one-dimensional (1D) species transport equations coupled with Onsager-Fuoss [33] and Debye-Huckel [34] models for ionic strength dependence on mobilities and ionic activities, respectively. Time-dependent simulations using SPRESSO are particularly useful for predicting transient behavior, such as analyte focusing during the startup and the transients of zone elongation due the shock interaction. However, for quicker estimates of increase in zone length

Table 1. Possible cationic ITP buffer systems that are compatible with bidirectional, cascade ITP.

	μ^0_{+1} ($\times 10^{-9}$ m^{2}V^{-1}s^{-1})	p$K_{a,+1}$
Cationic LE (LE+)		
Imidazole	52	7.15
2-Methyl pyridine	40.1	6.2
4-Methyl pyridine	40.1	6.1
Cationic TE (TE+)		
Bistris	26	6.4
Pyridine	30	5.18
Tris	29.5	8.07

These buffers effect large increase in zone lengths of anionic analytes upon shock interaction in bidirectional ITP. Listed are absolute mobilities of the cations and their acid dissociation constant.

in bidirectional ITP, we have also developed and used a steady-state solver based on a diffusion–free model of ITP [1,16]. The solver computes species concentrations in all bidirectional ITP zones by solving the moving boundary equations [2] (Hugoniot conditions across ITP shocks [16]) coupled with models for ionic strength effect on mobilities and acid dissociation constants [31]. We used both SPRESSO and this steady-state solver to design and analyze the processes described here. Unless otherwise stated, all simulations presented below are from SPRESSO. In the Supporting Information, we provide an outline of the steady-state solver and benchmark it against transient simulations using SPRESSO.

3.3 Simulation of cascade ITP process in bidirectional ITP

We performed simulations of the bidirectional, cascade ITP process for focusing, and separation of two model analytes using the SPRESSO simulation tool. For our simulations, we used 100 mM Mops as LE−, 20 mM Taurine as TE−, 280 mM Imidazole as LE+, 100 mM Bistris as TE+, and Hepes (S1−) and Tricine (S2−) as the model analytes. To illustrate the technique, we used a finite injection scheme for our simulations where S1− and S2− were initially present between the LE− and TE− zones. Further, we chose our initial conditions such that the analytes focused completely in plateau mode prior to shock interaction. This allowed us to quantify precisely the increase in zone length due to shock interaction. All simulations shown here take into account the effect of ionic strength on both mobilities and dissociation constants.

Figure 2A and B show the initial conditions of the simulation. Analytes S1− and S2− are placed between LE− and TE− zones. When electric field is applied, S1− and S2− focus and separate into distinct zones between LE− and TE−, as shown in Fig. 2C and D. Simultaneously, a cationic ITP shock (LE+/TE+ interface) interface forms between the LE+ and TE+ zones and propagates leftward. Behind the LE+/TE+ interface, the concentration of LE− drops significantly compared to its initial concentration (Fig. 2C). At the time LE+/TE+ interface meets the focused analytes, the high concentration LE− is completely replaced by the low concentration LE−. Because the analyte zone concentrations in ITP are proportional to the LE ion concentration, the interaction of cationic and anionic ITP shocks results in a decrease in zone concentrations of S1− and S2−. This readjustment of analyte zone concentrations is accompanied by simultaneous increase in their zone lengths. Figure 2E and F show this transition from high to low concentration LE−, where the S1− zone has partially readjusted to the lower concentration and S2− is still focused at high concentration. Figure 2G and H show the final state where both S1− and S2− are fully adjusted to new concentrations, and their zone lengths have increased (5-fold in this case) compared to those before the shock interaction. Also, the cationic ITP shock remains intact after the shock interaction and continues propagating leftwards.

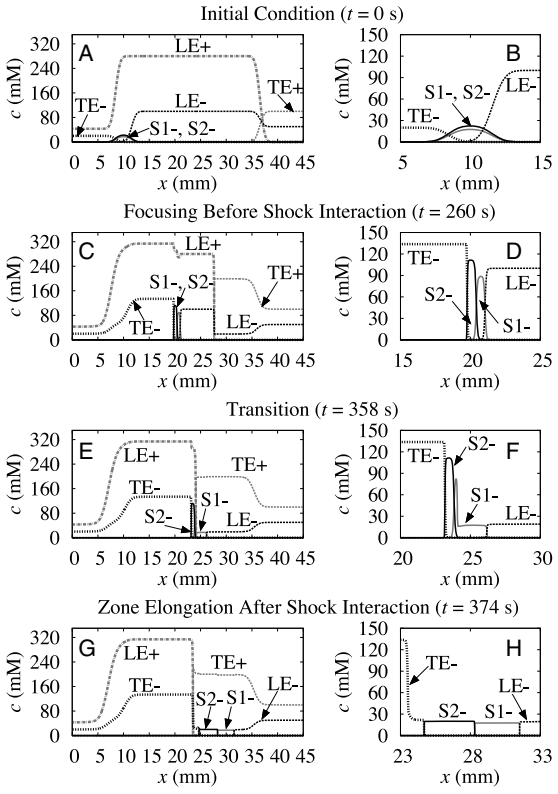

Figure 2. Simulation showing increase in zone length of anionic analytes using concentration cascade of LE− in bidirectional ITP. Plots in the second column are magnified views of species distributions shown in the first column. (A and B) The initial distribution of chemical species, prior to activating current. (C and D) The anionic and cationic ITP shocks shortly after application of electric field. (C) Anionic ITP shocks ($x = 20$ mm) propagating rightward and a cationic ITP shock ($x = 27$ mm) propagating leftward. (D) Anionic analytes S1− and S2− completely focused between LE− and TE− in narrow plateau zones. (E and F) The transition from high concentration LE− to low concentration LE− upon shock interaction. When the LE−/TE+ zone meets the focused analyte zones, it sets a new focusing condition for sample ions corresponding to a low LE− concentration. This forces S1− and S2− zones to readjust to lower concentrations, and this is accompanied by elongation of analyte zones (in accordance with conservation of species). (F) S1− zone readjusting to a lower concentration after interacting with the LE+/TE+ interface, while S2− zone is still at the previously adjusted higher concentration. (G and H) The final state in which analyte zones is fully adjusted to lower concentrations. (G) The LE−/S1− interface at $x = 32$ mm and the LE+/TE+ interface at $x = 24$ mm propagating toward the right and the left, respectively. (H) The fully elongated analyte zones that are five times longer than those prior to the shock interaction. Simulations were performed using our open source code SPRESSO [31, 32]. Chemistry is described in text. We assumed a constant current of 2 μA, and a D-shaped, wet-etched channel 90 μm wide, and 20 μm deep. We approximately account for electroosmotic flow as described in the text.

The simulation of cascade ITP process in bidirectional ITP shown in Fig. 2 itself highlights several advantages of our technique over conventional cascade ITP. As shown in Fig. 2C, the gradient in LE− concentration forms inside the

channel by simply applying an electric field. Our technique, therefore, eliminates integration of two or more channels containing different concentrations of LE− via valves or column coupling arrangements, as done in conventional cascade ITP. This in situ generation of cascade in LE ion concentration makes it possible to perform cascade ITP in a single channel, so it is easily accomplished in on- or off-chip systems. Further, in the current technique, the gradient in LE concentration remains sharp over time as it sweeps across the focused analyte zones. This well controlled, sharp gradient in LE ion concentration, which typically occurs over a distance of about 10 μm, provides us with a fast transition from focusing at high concentration LE to low concentration LE. This feature of our assay minimizes required channel lengths and assay time. These qualities are in contrast to conventional cascade ITP where the interface between high and low concentration LE diffuses over time and is susceptible to dispersive effects of nonuniform EOF and hydrodynamic flow. Hence, a complete readjustment of analyte zones to lower concentration LE is not achieved in conventional cascade ITP until the analyte zones completely migrate out of the dispersed region between the high and low concentration LE.

We also performed a simulation at conditions that allow experimental visualization of all bidirectional ITP zones. The results are shown in Fig. 3A. We used electrolyte chemistry similar to that used in Fig. 2, except here added a fluorescent NFT in trace concentration (25 μM) into the initial TE−/TE+ mixture. The NFT effective mobility was higher than all other anions. The NFT does not focus or disturb zone concentrations in bidirectional ITP, but its concentration quickly adapts to local electric fields in all zones. The NFT fluorescent intensity distribution therefore clearly delineates the various bidirectional ITP zones. In Section 3.4, we present corresponding experimental validation of this simulation (Fig. 3B) and discuss the NFT visualization technique in more detail.

Shown in Fig. 3A is a simulated spatiotemporal plot of fluorescent intensity of NFT during bidirectional cascade ITP. Here, the abscissa is the distance along the channel, the ordinate is time, and the scalar plotted is the fluorescent intensity of the NFT. To obtain the spatiotemporal plot from simulation, we neglect the effects of photobleaching and assumed a proportional relationship between the fluorescent intensity and the NFT concentration. Figure 3A shows zones of focused S1− and S2− ions propagating rightward, and a cationic ITP shock (LE+/TE+) shock propagating leftward. Since the NFT and LE− are both counterions for cationic ITP, their concentrations across the LE+/TE+ interface are in proportion to each other. The low fluorescent intensity in the LE−/TE+ zone compared to the LE−/LE+ zone, therefore, indirectly quantifies the manifold decrease in LE− concentration across the LE+/TE+ interface. When the anionic and cationic ITP shocks interact (25 s $< t <$ 45 s), the analyte zones readjust to lower concentrations (shown by the decrease in NFT intensity in the analyte zones) and achieve longer zone lengths. After the LE+/TE+ interface completely passes over the analyte zones ($t >$ 45 s), the zone lengths reach steady-state

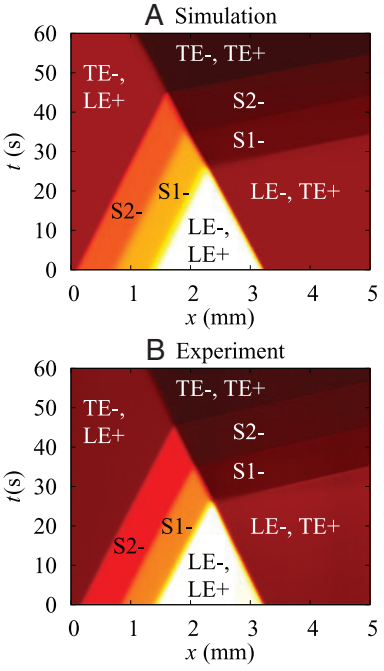

Figure 3. Numerical simulation and experimental visualization of increase in analyte zone length due to interaction of anionic and cationic ITP shocks. (A) Numerical simulation of propagating zones of anionic analytes (S1− and S2−) and a cationic ITP shock in bidirectional ITP. The spatiotemporal plot shows the intensity of a fluorescent nonfocusing tracer (NFT) versus the distance along the channel axis, *x*, and time, *t*. The NFT fluorescent intensity is inversely proportional to local electric field in each zone. (B) Experimental visualization of the same process using the fluorescent NFT technique [10]. Both (A) and (B) show anionic analyte zones and LE+/TE+ interface (cationic ITP shock) propagating toward the right and left, respectively. The LE+/TE+ interface meets the focused analyte zones near $x = 2.3$ mm and $t = 25$ s. Thereafter, analyte zones elongate by a factor of 5 and the LE+/TE+ interface continues migrating leftward (for $t > 25$ s). The elongation of analyte zones around $t = 25$ s is accompanied by increase in their migration speed (visible as decrease in slope of anionic ITP shocks). The electrolyte chemistry and electroosmotic mobility are the same as that in the simulation shown in Fig. 2, except we here mixed 25 μM Alexa Fluor 488 (NFT) in TE− to visualize ITP zones. Both simulations and experiments used a constant current of 2 μA, and a 53 mm long D-shaped, wet-etched channel 90 μm wide, and 20 μm deep.

values that are much greater than those before the shock interaction. For example, compare the width of the S2− at $t =$ 25 s (0.65 mm) with its width at 45 s (3.6 mm). Also, note the cationic ITP interface remains intact after its interaction with the analytes and continues propagating toward the left.

To take into an account the effect of electroomostic flow on the wave speeds in our simulations, we used the following approximate electroosmotic mobility dependence on conductivity (as suggested by the data in Ref. [35]): $\mu = \mu_r(\sigma_r/\sigma)^{1/3}$, where $\mu_r = 3 \times 10^{-10}$ $V^{-1}.m^2.s^{-1}$ and $\sigma_r = 0.5$ $S.m^{-1}$. The product $\mu_r\sigma_r^{1/3}$ is therefore the only fitting parameter used to match all experimentally measured shock speeds. (See Section 3.4 on experimental visualization of cascade ITP process in bidirectional ITP.)

3.4 Experimental visualization of increase in analyte zone length in bidirectional ITP

We performed visualization experiments to study and quantify the dynamics of the cascade ITP process in bidirectional ITP. For these experiments, we used finite injections of analytes in anionic ITP and visualized the effect on their zone lengths before, during, and after interaction with cationic ITP shock. We visualized the increase in zone lengths of focused analytes due to shock interaction in bidirectional ITP using the NFT technique [10]. In the NFT technique, fluorescent species that do not obey the ITP focusing conditions [36] are mixed with one or more of the ITP buffers in trace quantities. These fluorescent species do not focus in ITP, but their concentrations adapt to the local electric field and conductivity in different ITP zones. The fluorescent intensity of NFT, therefore, indicates the gradients in local conductivity across the ITP interfaces. For our experiments, we used 25 μM Alexa Fluor 488 (AF, an anionic dye) in the TE−/LE+ mixture as the NFT. In our experiments, AF is faster than all other anions and so does not focus. Further, anionic species cannot focus in the cationic ITP process. Hence, we visualized both anionic and cationic ITP zones in bidirectional ITP using AF as the lone NFT.

Figure 3B shows an experimentally measured spatiotemporal plot of the fluorescent intensity of NFT in bidirectional ITP with a concentration cascade of LE−. Like the simulated spatiotemporal plot (Fig. 3A), Fig. 3B shows a measured spatiotemporal plot showing the dynamics of the zones of focused analytes (S1− and S2−) before ($t < 25$ s), during (25 s $< t <$ 45 s), and after ($t > 45$ s) the shock interaction. The scalar quantity plotted (versus distance along channel axis and time) is the fluorescence intensity (from CCD images) in the channel averaged along the spanwise width of the channel. Our experimental visualizations compare well with the numerical simulations shown in Fig. 3A. First we capture qualitatively the dynamics of the entire process including propagation velocities of four shocks, their interactions, and the fluorescent intensity ratios across the shocks. We see clearly the rightward propagation of the focused sample zones S1− and S2− and the effect of interaction with the cationic shock. Compare the axial width of zones S1− and S2− prior to shock interaction (e.g., at $t =$ 20 s) to their width after shock interaction ($t > 45$ s). Quantitatively, our simulations predict ratios of the final to initial analyte zone lengths of 5.0 and 5.5 for S1− and S2−, respectively. Experimentally, we observe gains in zone length of 4.8 and 5.3 for S1− and S2−, respectively. Further, our simulations predict initial to final fluorescence intensity ratios of 7.0 and 8.4 for S1− and S2− zones, respectively, versus the observed values of 7.2 and 8.1. Importantly, these two parameters are independent of EOF mobility, and so each is predicted from first principles. By using a conductivity-dependent electroosmotic mobility as a single fitting parameter, we also accurately predict the time and the location of shock interactions and the eight observable shock speeds.

3.5 Effect of electrolyte chemistry on increase in zone length

We performed experiments to validate the dependence of analyte zone lengths on the electrolyte chemistry as given by the analytical model in Section 3.2 and by the diffusion-free model discussed earlier. According to the analytical model, for a given electrolyte chemistry, the ratio of the final to initial analyte zone lengths depends primarily on the ratio of LE+ to LE− concentrations in the initial LE−/LE+ mixture. For our experiments, we therefore kept the same LE−/LE+ chemistry but used seven ratios of LE+ to LE− concentrations ($c_{L+,init}/c_{L-,init}$) ranging from 2.0 to 3.2. The changes in composition of LE−/LE+ mixture were obtained by fixing the concentration of LE− at 100 mM and varying LE+ concentration from 200 to 320 mM. Figure 4A and C show the relative increase in zone length ($\Delta_{after}/\Delta_{before}$)of two analytes (Hepes and Tricine) due to shock interaction, for different proportions of LE+ in the LE−/LE+ mixture. The insets (Fig. 4B and D) show the same data, but here the ordinate is the inverse of the gain in zone length, i.e., $\Delta_{before}/\Delta_{after}$.

As predicted by the analytical model (Eq. (7), both experiments and calculations using the diffusion–free model show a linear decrease in $\Delta_{before}/\Delta_{after}$with increasing $c_{L+,init}/c_{L-,init}$. Correspondingly, the ratio of final to initial analyte zone lengths increases nonlinearly with increase in ratio of initial LE+ to LE− concentrations. As shown in Fig. 4A and C, the predictions of gain in zone length from the diffusion–free model agree well with the experimental observations. The predictions from analytical model agree qualitatively with experimental observations, but show significant differences in magnitude to the experimentally measured gain in zone length. As shown in Fig. 4A and C, the error in analytical predictions increases for larger gain in zone lengths (higher $c_{L+,init}/c_{L-,init}$). This error is a result of our assumption of negligible dependence of ionic strength on species mobilities in our analytical model. This conclusion is supported by fact that the analytical model compares well with the diffusion-free model if ionic strength effects are neglected in the latter (see Supporting Information). At high ionic strengths (around 100 mM), effective mobilities decrease considerably from the corresponding absolute mobility values (see Ref. [31]). This change in mobilities strongly affects gains in zone length as predicted by Eq. (7).

Here, we used the diffusion-free model along with ionic strength corrections for species mobilities to predict correctly the increase in zone lengths over wide range of LE−/LE+ compositions. We note that simulations using SPRESSO can alternatively be used for the same purpose, albeit at the expense of longer computational time (typically an order of magnitude longer than the diffusion-free model). In Fig. 4, we omit the results from SPRESSO simulations, as the differences between the predicted gain in zone lengths using the diffusion-free model and SPRESSO are negligible. However, we show their comparison in Supporting Information, where we benchmark the diffusion-free model against SPRESSO simulations.

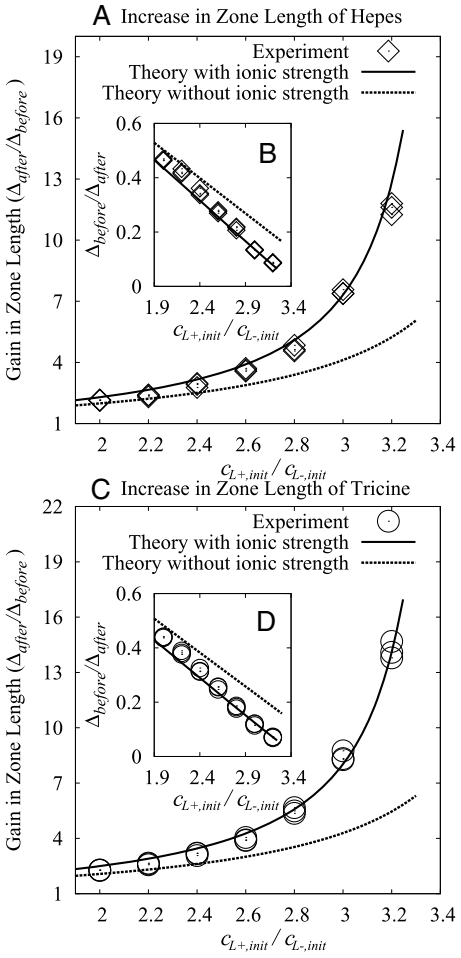

Figure 4. Effect of the leading electrolyte composition on gain in analyte zone lengths due to shock interaction. (A) and (C) The variation of measured and theoretical gain in zone length ($\Delta_{after}/\Delta_{before}$) of two analytes (Hepes and Tricine) versus the ratio of LE+ to LE− concentration in the initial LE+/LE− mixture ($c_{L+,init}/c_{L-,init}$). The gain in analyte zone length increases nonlinearly with increase in $c_{L+,init}/c_{L-,init}$. Both (A) and (C) show theoretical predictions with and without ionic strength correction for species mobility. Theoretical predictions that take into an account the effect of ionic strength on mobilities are in good agreement with experimental observations. Theoretical predictions from the analytical model (without ionic strength corrections) capture trends but underpredict gains in zone length. Insets (B) and (D) show the comparison with same data, but now the ordinate is the inverse of the gain in zone length ($\Delta_{before}/\Delta_{after}$). The simple analytical solution is useful for assay design and correctly predicts the linear variation of $\Delta_{before}/\Delta_{after}$ with $c_{L+,init}/c_{L-,init}$. LE− is Mops, LE+ is Imidazole, TE− is 20 mM Taurine, and TE+ is 100 mM Bistris. To vary the ratio $c_{L+,init}/c_{L-,init}$, we fixed the concentration of LE− at 100 mM and varied the concentration of LE+ from 200 to 320 mM. We visualized different ITP zones using Alexa Fluor 488 as a fluorescent NFT. All theoretical results use the same conditions.

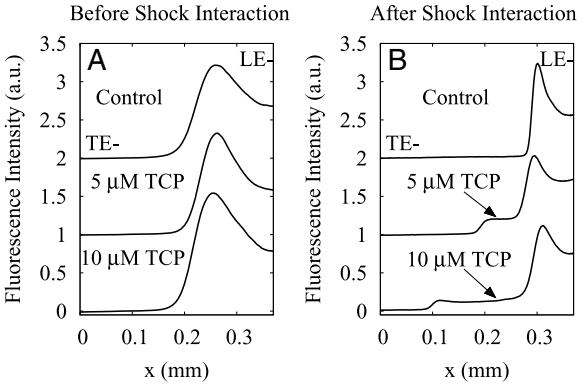

Figure 5. Indirect fluorescence detection of 5 μM 2,4,6-trichlorophenol (TCP) using the NFT technique with concentration cascade of LE−. (A) The fluorescent intensity of NFT (Alexa Fluor 488) prior to the interaction of the cationic and anionic ITP shock waves. Before shock interaction, the control experiment in the absence of TCP shows a single upward step in the fluorescent intensity from TE− to LE−. When TCP is mixed with TE− at concentrations of 5 and 10 μM, the fluorescence signal before the shock interaction does not change appreciably. At these conditions, TCP is focused in peak mode and so has negligible effect on the background electric field. (B) The fluorescence intensity of NFT after the shock interaction. For the cases where 5 and 10 μM TCP are present in TE−, we observe a distinct step in NFT signal after the shock interaction. Thus, TCP that focuses in peak mode before the shock interaction, transitions to plateau mode after the interaction of anionic and cationic ITP shock waves. We observed a signal overshoot at the boundary of the LE− zone (see text). For these experiments, we used a constant potential of 500 V across a 53 mm long, D-shaped, wet-etched channel 90 μm wide, and 20 μm deep.

3.6 Demonstration of high-sensitivity detection using bidirectional ITP

Lastly, we used bidirectional ITP with concentration cascade of LE− for high-sensitivity detection of TCP, a carcinogenic pollutant [37]. For these experiments, we used 150 mM Mes as LE−, 20 mM Hepes as TE−, 470 mM Imidazole as LE+, and 300 mM Bistris as TE+. Our simulations predict approximately 20-fold increase in zone length due to shock interaction with this electrolyte chemistry. To increase the sample loading, we performed semi-infinite injection of TCP by mixing it with anionic TE (TE−/LE+ mixture). Figure 5A and B show measured isotachopherograms obtained before and after the shock interaction. For the control experiment, where no TCP was present in the TE−/LE+ mixture, we observe a single step in the NFT signal corresponding to the LE−/TE− interface. When TCP is spiked in anionic TE at concentrations of 5 and 10 μM, the signal prior to shock interaction is unchanged. At these low concentrations, TCP is focused in peak mode and so its zone length is on the order of LE−/TE− interface thickness. However, in the same experiments, the TCP zone length increases upon its interaction with the cationic ITP shock. Figure 5B shows well-resolved plateau zones of TCP after the shock interaction. As expected, the TCP zone lengths are proportional to the initial amount of TCP in the anionic TE.

We note that we observed in these experiments a signal overshoot at the boundary of LE− zone. Similar overshoots have been observed in other ITP systems [36, 38], including those with the NFT technique [10]. However, we note this

signal overshoot does not here affect our ability to detect and quantify the length of the TCP zone. The detection sensitivity of our technique is currently in the micromolar range. We estimate that the sensitivity can be further increased by at least a factor of approximately 50 by using other techniques in concert with our bidirectional cascade ITP method, including variation of channel cross-section [15, 16] and hydrodynamic counterflow [14].

4 Concluding remarks

We developed a new method to create concentration cascade of LE in ITP by leveraging interaction of anionic and cationic shock waves in bidirectional ITP. We described how bidirectional ITP with approaching and interacting shock waves can be used to focus analytes and simultaneously create a gradient in LE ion concentration across a counterionic ITP shock wave. We used this feature of bidirectional ITP to initially focus analytes using a high concentration of LE ions. Shock interaction then causes a decrease in the LE ion concentration ahead of focused analytes. The high LE ion concentration prior to the shock interaction increases the sample loading capacity. The subsequent, lower concentration of LE ions established by the shock interaction increases the detection sensitivity by enforcing longer analyte zones. To the best of our knowledge, this is the first time where cascade ITP has been performed by generating in situ gradient in LE concentration using only the initial condition of the chemistry.

We presented an analytical model to predict the gain in analyte zone length due to shock interaction. Based on the analytical model, we discussed practical choices of electrolyte chemistries for maximizing the detection sensitivity. To illustrate the dynamics of analyte zone elongation, we performed detailed numerical simulations of 1D electromigration diffusion equations. We validated the simulations using visualizations based on indirect fluorescence of bidirectional ITP zones. Our simulations predict accurately (and from first principles) the local zone concentrations and the gain in analyte zone length due to shock interaction. By further incorporating a single fitting parameter for electroosmotic mobility, the simulations also correctly predict the dynamics of shock wave propagation in bidirectional ITP before, after, and during the shock wave interaction. We performed a series of controlled bidirectional ITP experiments to demonstrate the effect of varying proportion of cationic to anionic LE concentrations on the gain in zone length of anionic analytes. Our experiments show that the gain in zone length of anionic analytes due to shock interaction increases with increase in ratio of cationic to anionic LE concentrations. Similar behavior is predicted qualitatively by our analytical model and more precisely by numerical simulations. Based on these results, we designed a bidirectional ITP chemistry to demonstrate a factor of 20 increase in detection sensitivity of TCP.

Bidirectional ITP with interacting shock waves is an elegant way of triggering a wide range of modifications to ITP processes. Here, we demonstrated cascade ITP for high-sensitivity detection using bidirectional ITP. Our process eliminates the requirement of physical separation of high and low concentration LEs using valves or a column coupling arrangements. Unlike conventional implementations of cascade ITP, the LE concentration gradient in our technique is generated in situ, and this allows its integration in a single channel such as in standard CE equipments. Furthermore, the technique can be easily applied in concert with hydrodynamic counterflow and/or converging channel cross-sections to further enhance detection sensitivity.

S.S.B. is supported by a Mayfield Stanford Graduate Fellowship and a Kodak Fellowship. We gratefully acknowledge funding from the Defense Advanced Research Projects Agency (DARPA) under grant number N660001-09-C-2082, and the DARPA sponsored Micro/Nano Fluidics Fundamental Focus (MF3) under contract number N66001-10-1-4003.

The authors have declared no conflict of interest.

5 References

[1] Everaerts, F. M., Beckers, J. L., Verheggen, Th. P. E. M., *Isotachophoresis-Theory, Instrumentation and Applications*, Elsevier, Amsterdam 1976.

[2] Bocek, P., *Top. Curr. Chem.* 1981, *95*, 131–178.

[3] Zhukov, M. Y., *U.S.S.R. Comput. Math. Math. Phys.* 1984, *24*, 138–149.

[4] Ermakov, S. V., Zhukov, M. Y., Capelli, L., Righetti, P.G., *Electrophoresis* 1998, *19*, 192–205.

[5] Khurana, T. K., Santiago, J. G., *Anal. Chem.* 2008, *80*, 6300–6307.

[6] Chen, S., Graves, S. W., Lee, M. L., *J. Microcol. Sep.*1999, *11*, 341–345.

[7] Bercovici, M., Kaigala, G. V., Backhouse, C. J., Santiago, J. G., *Anal. Chem.* 2010, *82*, 1858–1866.

[8] Zemann, A. J., Schnell, E., Volgger, D., Bonn, G. K., *Anal. Chem.* 1998, *70*, 563–567.

[9] Ludwig, M., Kohler, F., Belder, D., *Electrophoresis* 2003, *24*, 3233–3238.

[10] Chambers, D., Santiago, J. G., *Anal. Chem.* 2009, *81*, 3022–3028.

[11] Khurana, T. K., Santiago, J. G., *Anal. Chem.* 2008, *80*, 279–286.

[12] Bercovici, M., Kaigala, G. V., Backhouse, C. J., Santiago, J. G., *Anal. Chem.* 2010, *82*, 1858–1866.

[13] Garcia-Schwarz, G., Bercovici, M., Marshall, L. A., Santiago, J. G., *J. Fluid Mech.* 2011, *679*, 455–475.

[14] Everaerts, F. M., Vacik, J., Verheggen, Th. P. E. M., Zuska, J., *J. Chromatogr.* 1970, *49*, 262–268.

[15] Everaerts, F. M., Verheggen, T. P., Mikkers, F. E., *J. Chromatogr.* 1979, *169*, 21–38.

[16] Bahga, S. S., Kaigala, G. V., Bercovici, M., Santiago, J. G., *Electrophoresis* 2011, *32*, 563–572.

[17] Bottenus, D., Jubery, T. K., Dutta, P., Ivory, C., *Electrophoresis* 2011, *32*, 550–562.

[18] Bottenus, D., Jubery, T. K., Ouyang, Y., Dong, W., Dutta, P., Ivory, C. F, *Lab. Chip* 2011, *11*, 890–898.

[19] Bocek, P., Deml, M., Janak, J., *J. Chromatogr.* 1978, *156*, 323–326.

[20] Mikkers, F. E. P., Everaerts, F. M., Peek, J. A. F, *J. Chromatogr.* 1979, *168*, 293–315.

[21] Kohlrausch, F., *Ann. Phys. Chem.* 1897, *298*, 209–239.

[22] Alberty, R. A., *J. Am. Chem. Soc.* 1950, *72*, 2361–2367.

[23] Kaniansky, D., Masar, M., Bielcikova, J., Ivanyi, F., Eisenbeiss, F., Stanislawski, B., Grass, B., Neyer, A., Johnck, M., *Anal. Chem.* 2000, *72*, 3596–3604.

[24] Oshurkova, O. V., Gorshkov, A.I., *Russ. Chem. Rev.* 1993, *62*, 729–742.

[25] Oshurkova, O. V., Gorshkov, A.I., Nesterov, V. P., *Russ. J. Electrochem.* 2004, *40*, 516–520.

[26] Bahga, S.S., Chambers, R.D., Santiago, J.G., *Anal. Chem.* 2011, *83*, 6154–6162.

[27] Jovin, T. M., *Biochemistry* 1973, *12*, 871–879.

[28] Oshurkova, O. V., Ivanova, I. A., *Dokl. Akad. Nauk. SSSR* 1976, *227*, 1371–1374.

[29] Persat, A., Suss, M. E., Santiago, J. G., *Lab Chip* 2009, *9*, 2454–2469.

[30] Porras, S. P., Riekkola, M., Kenndler, E., *Electrophoresis* 2003, *24*, 1485–1498.

[31] Bahga, S.S., Bercovici, M., Santiago, J. G., *Electrophoresis* 2010, *31*, 910–919.

[32] Bercovici, M., Lele, S. K., Santiago, J. G., *J. Chromatography. A* 2009, *1216*, 1008–1018.

[33] Onsager, L., Fuoss, R. M., *J. Phys. Chem.* 1932, *36*, 2689–2778.

[34] Debye, P., Huckel, E., *Physik. Z.* 1923, *24*, 305–325.

[35] Bharadwaj, R., Santiago, J. G., *J. Fluid Mech.* 2005, *543*, 57–92.

[36] Gebauer, P., Bocek, P., *J. Chromatography* 1983, *267*, 49–65.

[37] Gowda, T. P. H., Lock, J. D., Kurtz, R. G., *Water Air Soil Poll.* 1985, *24*, 189–206.

[38] Bocek, P., Gebauer, P., Deml, M., *J. Chromatogr.* 1981, *217*, 209–224.

